SCIENTIFIC REPORTS

OPEN

Enhanced stability of freestanding lipid bilayer and its stability criteria

Dae-Woong Jeong[1], Hyunwoo Jang[1], Siyoung Q. Choi[2] & Myung Chul Choi[1]

We present a new strategy to dramatically enhance the stability of freestanding lipid bilayers. We found that an addition of a water in oil emulsion stabilizer, SPAN 80 to a solvent phase guarantees nearly millimeter-scale stable freestanding lipid bilayers. The water permeability, bilayer area, contact angle, and interfacial tension were measured as a function of time and SPAN 80-to-lipid weight ratio ($\Phi_{SPAN\ 80}$) with several different solvents. Surprisingly, the SPAN 80, instead of remaining in the bilayer, was moved out of the bilayer during the bilayer formation. Also we studied the effect of solvent on freestanding bilayer formation, and found that squalene was the only solvent that was not incorporated into the bilayer. The regime of stable bilayer formation was experimentally determined to be $3/1 < \Phi_{SPAN\ 80} < 15/1$, and we suggest general stability criteria for bilayer formation. This technique and the suggested stability criteria can be potentially helpful to many model membrane-based researches in life sciences, physical sciences and biomedical engineering fields.

Engineering artificial model cell membranes, such as lipid vesicles[1,2], supported lipid bilayers[2–5], and freestanding lipid bilayers[6–24], is an important issue in physical science, life science and biomedical engineering[25,26]. Such model membranes can provide a useful *in vitro* platform for studying a variety of biological problems related to cell membranes[27,28]. Of those, freestanding lipid bilayers have advantages over other techniques in that both sides of the lipid bilayer can be under the control of various physicochemical parameters, including ionic strength and pH, chemical and biological molecules. In particular, freestanding lipid bilayers with large area ($\geq$several hundred μm) and horizontally planar geometry would enable important problems to be tackled such as the direct visualization of structures, phase behaviors[29–32], dynamic behaviors[33], and interactions of complex systems (e.g. membrane proteins, lipid rafts, nanoparticles, other vesicles) in a simplified model cell membrane[14,15,18,24].

The challenge in the formation of freestanding lipid bilayers is their poor stability. Accordingly, a lot of new fabrication methods for stable freestanding lipid bilayers have been introduced[6–22]. Recently, an excellent technique, termed as droplet interface bilayers (DIBs) was developed[18–23] where two lipid-coated water droplets immersed in solvent bring together to form a stable freestanding lipid bilayer with large area. The DIBs can be used for imaging experiments and easily incorporate membrane proteins with simple fabrication process. Notably, Wallace and coworkers recently developed a model lipid bilayer by placing a lipid-coated droplet on top of a lipid-coated agarose gel to enhance its stability, while taking advantage of horizontally planar geometry for imaging experiments[21,22].

In this paper, we introduce a new strategy to dramatically enhance stability of DIBs by using water in oil (W/O) emulsion stabilizer, SPAN 80. Our lipid bilayer is also horizontally planar as others[21,22], but it is formed on top of water instead of agarose gel. Figure 1 shows the schematic illustration of how a freestanding DIB is formed, and provides the corresponding microscopy images of freestanding lipid bilayer formation, monitored by side-view microscope. We prepared a planar interface between water and squalene in which lipids and SPAN 80 were dissolved. The lipids and SPAN 80 are spontaneously adsorbed to the interface, forming a planar monolayer. A water droplet with a size range of 100–500 μm in diameter was introduced into the squalene, where the other monolayer was formed at the spherical water droplet. As a lipid coated water droplet approaches a plane interface, the solvent phase between the interfaces drains out and the two monolayers undergo a "zipping" process during which the two monolayers adhere to each other[14–23,34], resulting in a horizontally planar freestanding lipid bilayer. Our control parameter was the SPAN 80-to-lipid weight ratio $\Phi_{SPAN\ 80}$ (with a constant lipid concentration of 1 mg/ml), which determines the squalene/water interfacial tension.

[1]KAIST, Department of Bio and Brain Engineering, Daejeon, 34141, Korea. [2]KAIST, Department of Chemical and Biomolecular Engineering, Daejeon, 34141, Korea. Correspondence and requests for materials should be addressed to S.Q.C. (email: sqchoi@kaist.ac.kr) or M.C.C. (email: mcchoi@kaist.ac.kr)
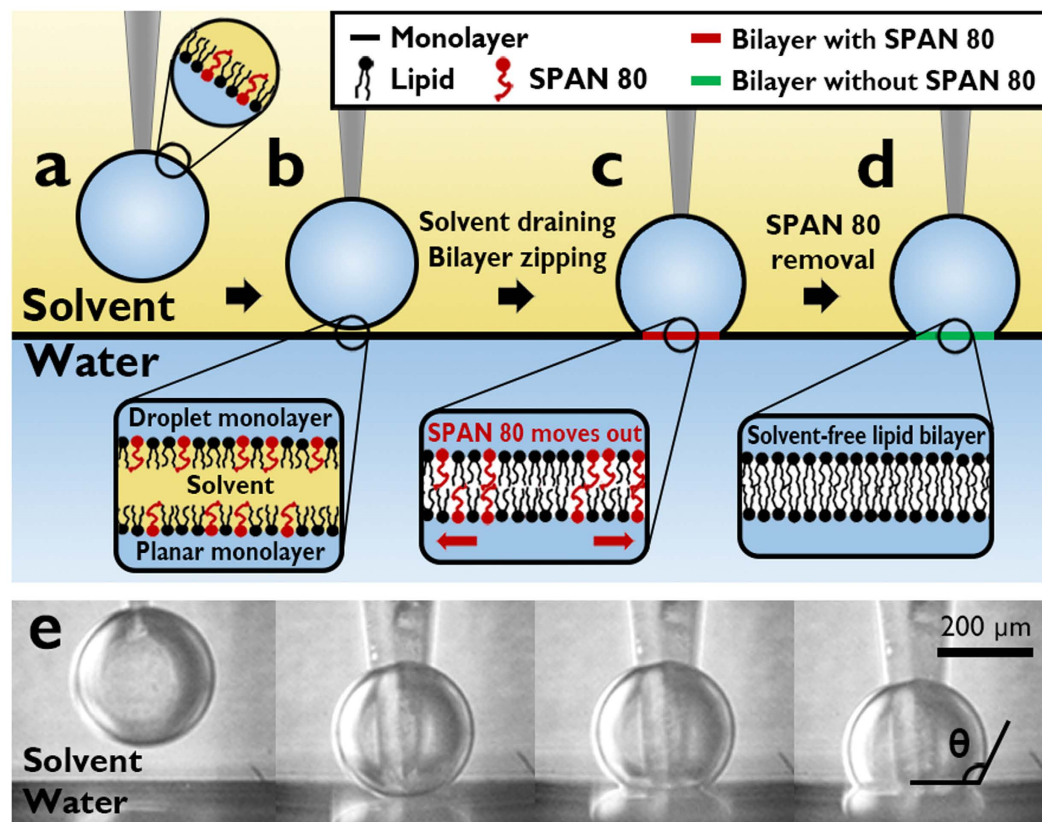
Figure 1. Schematics illustrating the formation of freestanding bilayer with enhanced stability and the side-view microscope images. (a) A lipid coated water droplet in squalene (i.e. droplet monolayer) approaches to a lipid adsorbed solvent/water interface (i.e. planar monolayer). **(b)** Solvent drains out and then two monolayers start zipping to form bilayer. **(c)** During (or after) bilayer formation, SPAN 80 is moved out of the bilayer driven by the adhesion of two monolayers. **(d)** The freestanding bilayer with large area, planar geometry and solvent & SPAN 80-free is formed. **(e)** Side-view microscopy images in correspondence with each of **(a–d)**. Scale bar: 200 μm.

Results and Discussion

Interestingly, in all our experiments, the freestanding bilayers remained stable at least for several days without changes in the bilayer area or contact angle for an appropriate range of Φ_{SPAN80} whereas a droplet immediately coalesced for too low Φ_{SPAN80}. This implies that the SPAN 80 dramatically enhances the stability of freestanding lipid bilayer[18,20–23]. Such enhancement in stability of the freestanding bilayer can be explained by the role of SPAN 80 during the impact of the two monolayers which include the following. First, it modifies the spontaneous curvature; its hydrophobic tail is bulky relative to the hydrophilic head, which induces negative spontaneous curvature. For the bilayer with low stability, a transient pore, which is hydrophilic pore through the bilayer with highly positive curvature, is formed before merging of droplet into sub-phase water. The SPAN 80 with negative curvature plays a critical role for preventing the formation of transient pore to stabilize bilayer[35]. Second, it modifies the interfacial tension. As Φ_{SPAN80} increases, the interfacial tension decreases, thus it reduces the energetic benefit of droplet coalescence[35]. We also checked other surfactants such as oxidized squalene and docosahexaenoic acid (DHA) that have similar molecular shapes significantly enhance the stability of lipid bilayers. In the previous study, this level of stability was achieved only when the limited kinds of lipid (e. g. 1,2-diphytanoyl-sn-glycero-3-phosphocholine, DPhPC) with exceptionally bulky tail or solvent (e. g. hexadecane) remaining in the bilayer after zipping process are used, and this result indicates that the SPAN 80 dramatically enhances stability of the freestanding lipid bilayer[18,20–23].

It was expected that our bilayers would be composed of a mixture of lipid and SPAN 80. However, we surprisingly found that SPAN 80 is likely to be moved out of the bilayer during/after the bilayer formation. To systematically verify the removal of SPAN 80 from the bilayer, we measured the bilayer area, contact angle, bilayer tension, and adhesion energy of two monolayers of dimyristoylphosphatidylcholine (DMPC) and dioleoylphosphatidylcholine (DOPC). We performed all of our experiments at 25 °C where both lipids exhibit a liquid disordered phase[36]. Figure 2(a,b) is the plot of the bilayer area and the contact angle of the freestanding bilayer as a function of time. At t = 0, the bilayer area is of the same diameter d ≈ 220 μm for both DOPC and DMPC. For DMPC, a drastic change in the bilayer area and the contact angle (θ) occurs at t < 200 sec, followed by the constant values d = 523 μm and θ = 56°, whereas for DOPC, the bilayer area and contact angle remain unchanged. Figure 2(c) shows the interfacial tension of the bilayer γ_B of DOPC and DMPC at Φ_{SPAN80} = 5/1. The bilayer interfacial tension
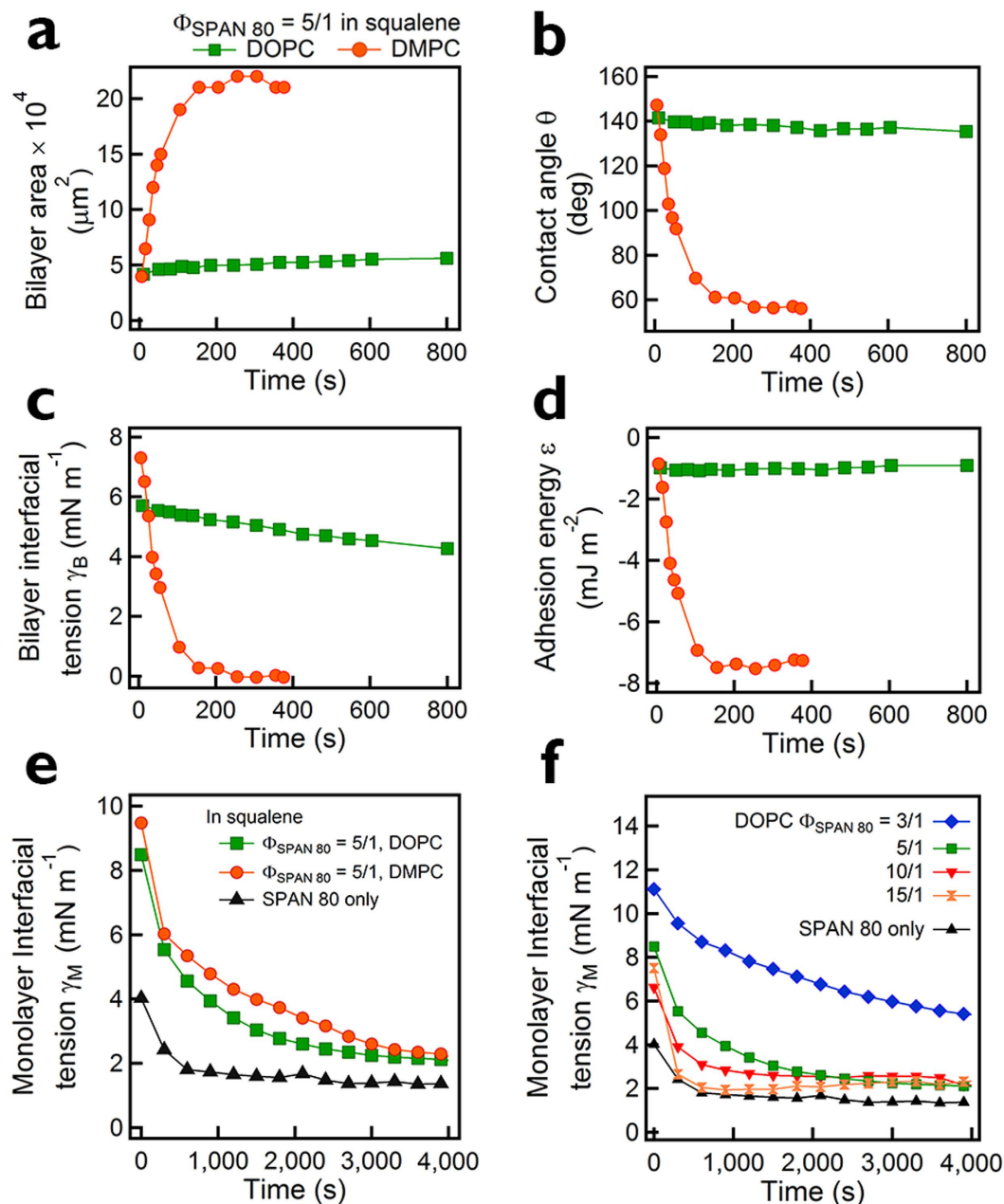
Figure 2. For the freestanding DOPC and DMPC bilayers in squalene at $\Phi_{SPAN80} = 5/1$, plots of Bilayer area (**a**), Contact angle (**b**), Interfacial tension (**c**), and Adhesion energy (**d**) vs. time. The t = 0 is when the bilayers are formed. (**e**) Monolayer interfacial tension vs. time for DOPC and DPPC at SPAN 80-to-lipid weight ratio (Φ_{SPAN80}) of 5/1, and for SPAN 80 only. (**f**) Monolayer interfacial tension vs. time as a function of Φ_{SPAN80}.

is defined as the sum of the interfacial tension of monolayers on droplet surface and planar interface: Young's equation $\gamma_B = \gamma_M (1 - \cos\theta)$, where γ_M and γ_B are the interfacial tensions of the monolayer and the bilayer, respectively. Monolayer interfacial tension was measured by using a pendant drop technique as shown in Fig. 2(e) and (f)[37]. Both DOPC and DMPC have similar γ_M, but γ_B of DOPC (4.3–5.7 mN/m) is far greater than γ_B of DMPC ($\sim$0 mN/m at t > 200 sec). Figure 2(d) shows the adhesion energy per unit area, $\varepsilon = \gamma_B - 2\gamma_M$ (in J/m^2), of the DOPC and DMPC bilayer at $\Phi_{SPAN80} = 5/1$. The equilibrium adhesion energy is -1.0 mJ/m^2 (DOPC) and -7.4 mJ/m^2 (DMPC).

The increase in the adhesion energy over time suggests that the bilayer composition changes after bilayer formation. When only SPAN 80 was used without any lipid, no adhesion was observed, implying that zero adhesion exists between SPAN 80 molecules. Therefore, to maximize the adhesion (to lower the energy), lipid molecules should go into the bilayer, excluding SPAN 80 out of the bilayer. At the same time, this demixing process of lipid and SPAN 80 results in an entropic penalty, more specifically, the entropy of mixing. In other words, the competition between adhesion energy and the entropy of mixing determines the distribution of SPAN 80.
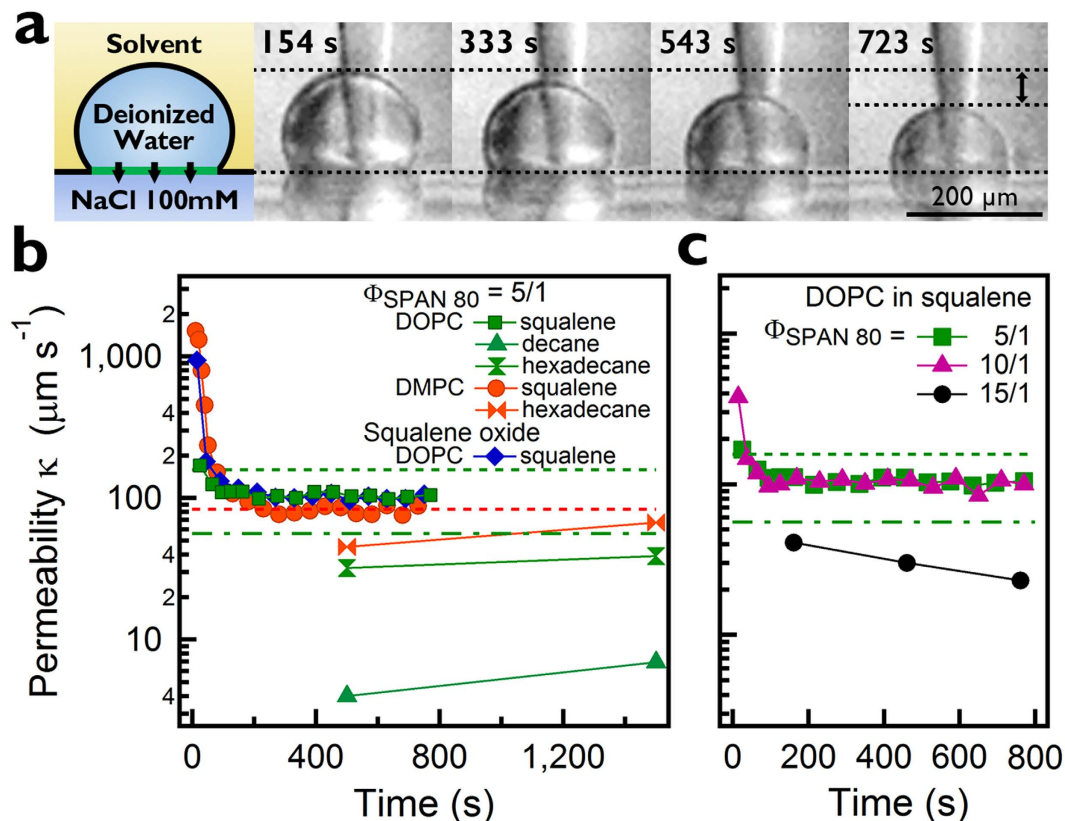
Figure 3. Water permeability of freestanding bilayers. (**a**) Side-view microscopy images show the decrease in the volume of droplet as water transports through the lipid bilayer by osmotic pressure gradient (100 mM NaCl at the bottom phase). (**b,c**) Water permeability vs. time, for DOPC and DMPC bilayer for different stabilizers (SPAN 80 and squalene oxide) and solvents (squalene, decane and hexadecane) (**b**) and for DOPC in squalene at different $\Phi_{SPAN\,80}$ = 5/1, 10/1, 15/1 (**c**). The values from the previous works of $\kappa = 83 \pm 7.6\,\mu$m/sec for DMPC (dotted line in red), and $\kappa = 56 \pm 9$ and $158 \pm 5.8\,\mu$m/sec for DOPC (dash-dot and dotted lines in green) are shown[39,40].

For the DOPC and DMPC bilayer at Φ_{SPAN80} = 5/1, the estimated entropic penalty of SPAN 80 is at most in the same order of magnitude as the energetic gain obtained by introducing more lipids in the bilayer region (see Supplementary Figure S3). Therefore, the decrease in the bilayer interfacial tension for DMPC at an early stage (t < 200 sec) in Fig. 2(c) supports that SPAN 80 is removed from the bilayer, to increase adhesion between the two monolayers, as seen in Fig. 2(d). During this period, SPAN 80 is removed from the lipid bilayer and the interfacial tension of the DMPC bilayer drops into the plausible range, when compared with the bilayer rupture tension γ_{br} (DMPC) ≈ 2.7 mN/m (at least, the bilayer tension should be smaller than the rupture tension). γ_B of DOPC (4.3–5.7 mN/m) is also less than γ_{br} (DOPC) ≈ 10.2 mN/m[38].

Another evidence that SPAN 80 is likely to be removed from the bilayer is shown in Fig. 3, the water permeability measurement. The 100 mM NaCl dissolved in the bottom water of the plane interface generates osmotic gradients across the bilayer, resulting in water transport through the lipid bilayer membrane (Fig. 3(a)). We measured the volume change in the water droplet as a function of time[19,20]. In Fig. 3(b), the water permeability of both the DMPC and DOPC bilayer at Φ_{SPAN80} = 5/1 decreases from 1521.3 μm/sec (DMPC) and 169.7 μm/sec (DOPC) to reach constant values of $83.0 \pm 6.0\,\mu$m/sec (DMPC) and $103.6 \pm 4.2\,\mu$m/sec (DOPC) after the bilayer formation. This equilibrium permeability is in good agreement with the previous measurements: $83 \pm 7.6\,\mu$m/sec for DMPC, 56 ± 9 and $158 \pm 5.8\,\mu$m/sec for DOPC[39,40]. The initial decrease in water permeability is consistent with the adhesion measurement and thus is most likely due to the process of removing SPAN 80 from the bilayer. Moreover, this initial decrease in water permeability is similarly shown for different stabilizer, squalene oxide, and values of the equilibrium permeability are almost identical ($102.6 \pm 6.0\,\mu$m/sec for squalene oxide) no matter what kind of stabilizer is used. This suggests that the freestanding bilayer at equilibrium might be composed of DOPC (or DMPC) lipid only.

The permeability result (Fig. 3(b)) also implies that our freestanding bilayer is squalene-free since this is consistent with the measurement for lipid vesicle that has no solvent in it. It is also widely known that squalene does not invade into bilayers or in between two monolayer leaflets[6–9,21,22]. Decane and hexadecane exhibit a lower permeability in comparison with squalene. A previous study reported that decane and hexadecane remain in the lipid bilayer after the formation of DIB[21,22]. When the bilayer contain a solvent such as decane or hexadecane, water molecules will cross the solvent layer in addition to the lipid bilayer, which results in drops in the water
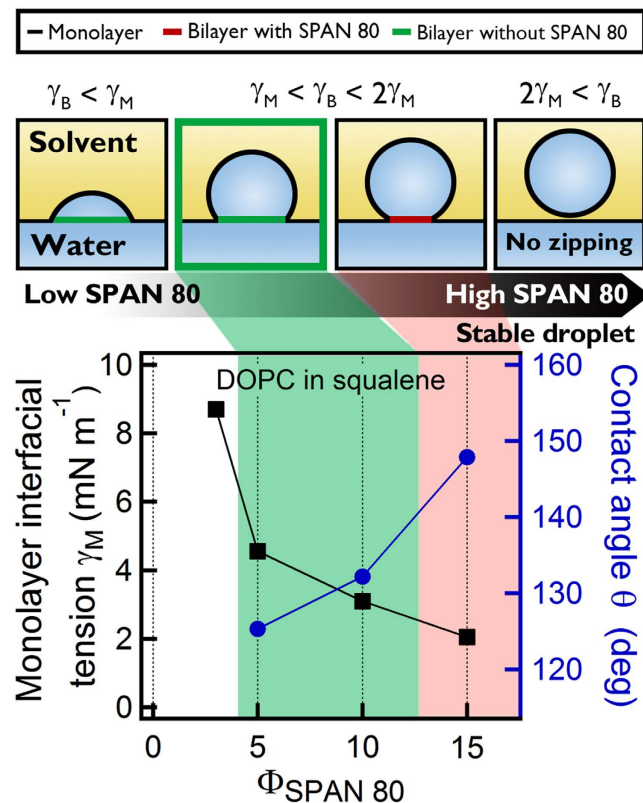
Figure 4. Stability criteria for freestanding bilayer formation. Monolayer interfacial tension for DOPC as a function of SPAN 80-to-lipid weight ratio Φ_{SPAN80} (symbol in black square, left axis). Contact angle is plotted in the right axis (in blue circle). The regime of stable and SPAN 80-free bilayer is shown in green. For higher Φ_{SPAN80}, SPAN 80 is remained in the bilayer due to low adhesion, and for lower Φ_{SPAN80}, SPAN 80 does not reduce the interfacial tension enough to form a stable bilayer.

permeability. The interfacial tension of freestanding bilayer is 6.7–11.4 mN/m in decane, and 7.0–10.4 mN/m in hexadecane, which are significantly higher than the 4.3–5.7 mN/m in squalene (see Supplementary Figure S5). We note that the interfacial tensions of both decane and hexadecane are around the rupture tension of the DOPC bilayer ($\approx$10.2 mN/m) in the absence of solvents.

In Fig. 3(c), the water permeability vs. time as a function of SPAN 80-to-DOPC weight ratio $\Phi_{SPAN\ 80}$, shows the concentration dependent role of SPAN 80 in the formation of the freestanding lipid bilayer. The bilayer zipping occurs at $\Phi_{SPAN80} > 3/1$ (at $\Phi_{SPAN80} = 0$ and 3/1, the bilayer formation fails, i.e. a droplet coalesces to water phase). For both $\Phi_{SPAN80} = 5/1$ and 10/1, the same permeability $\kappa = 98\,\mu m/sec$ is measured. For $\Phi_{SPAN80} = 15/1$, however, the permeability is 2.4–4.3 fold smaller ($\kappa = 23$–41 $\mu m/sec$). From this result, we conclude that the regime $3/1 < \Phi_{SPAN80} < 15/1$ is the condition under which a stable and solvent-free freestanding bilayer of DOPC in squalene can be formed.

Combining all the results above, we set up stability criteria for SPAN 80 stabilized bilayer formation (Fig. 4). At very low Φ_{SPAN80}, SPAN 80 does not reduce the interfacial tension enough to form a stable bilayer, and thus coalescence immediately occurs as soon as a droplet is in contact with the planar surface. For sufficiently high Φ_{SPAN80}, the interfacial tension is low enough for stable bilayers, exhibiting the successful zipping process with the intermediate contact angle between 90° and 180°. For very high Φ_{SPAN80} (in a case of $2\gamma_M < \gamma_B$), however, the contact angle reaches 180°, and the adhesion does not occur. Even if the contact angle does not reach 180°, too high Φ_{SPAN80} reduces adhesion between the two monolayers, and in this case, the entropy of mixing is too big to increase the adhesion, leaving some SPAN 80 in the bilayer. Moreover, the regulation of interfacial tension directly affects the three phase contact angle of the lipid bilayer: two lipid monolayers and a bilayer. The importance of the interfacial tension regulation is easily seen in the DMPC bilayer formation. For DMPC, the interfacial tension of the lipid bilayer is nearly zero. The DMPC monolayer interfacial tension is also low enough, so it appears to form a stable bilayer at first. However, the contact angle of the lipid bilayer changes over time, and eventually becomes very low (<60°), and the abrupt change at the kink seems to make the bilayer unstable. The stability of the DMPC bilayer becomes worse if the contact angle is very low. Therefore, to enhance the stability of the bilayer and to simultaneously obtain solvent-free and SPAN 80-free bilayers, there is an appropriate and optimum range of Φ_{SPAN80}. Since different lipid species show different lipid bilayer interfacial tension, to form stable freestanding lipid bilayer this proper range of Φ_{SPAN80} will change. We also should note that previous DIBs use higher concentrations of lipids that might have an appropriate interfacial tension[18–23].

Conclusion

We demonstrated a new strategy to dramatically enhance stability of DIB with a large area, planar and solvent-free as well by using W/O emulsion stabilizer, SPAN 80. Surprisingly, SPAN 80 is most likely to be moved out of the bilayer, maximizing the adhesion of the lipid monolayers, and overcoming the entropy of mixing penalty. This removal of SPAN 80 was demonstrated by time-dependent adhesion and permeability experiments. We also showed that the freestanding bilayer fabricated by our technique is squalene-free as well. We finally suggested stability criteria for the SPAN 80 stabilized freestanding bilayer formation, involving the regulation of interfacial tension by controlling SPAN 80 concentration. This stabilization strategy can be universally applied to various freestanding bilayer formation techniques such as the conventional DIBs and the traditional black lipid membranes.

Methods

Dimyristoylphosphatidylcholine (DMPC), dioleoylphosphatidylcholine (DOPC) and SPAN 80 are purchased. Squalene oxide is prepared by direct light exposure on squalene for four days with air contact. We use deionized water for all of our experiments. The imaging experiments were performed by using homebuilt side-view microscope. The sample of phospholipid (DMPC or DOPC) in chloroform is contained in glass vial and dried in vacuum. SPAN 80 dissolved in squalene is added into the dried phospholipid, and then sonicated for 30 minutes. We prepare a trough filled with water, and the phospholipid solution is placed on top of water to form a planar squalene/water interface. The glass capillary of 0.78/1.0 mm in inner/outer diameter respectively is tapered to 10 μm of diameter by a micropipette puller. The capillary is filled with water and then mounted to the micro-injector. The capillary tip is placed above the squalene/water interface. By applying a pressure of ~100 hPa, the droplet of ~300 μm diameter is introduced right above the planar interface. Both planar and droplet squalene/water interfaces are incubated for over 10 minutes for the adsorption of phospholipid and SPAN 80 monolayers, which are termed as planar monolayer and droplet monolayer, respectively. The droplet is moved toward the planar interface until the droplet gently touches the planar interface. After a few minutes of waiting, two monolayers undergo "zipping" process, in result, form the lipid bilayer between two water phases. The size of freestanding lipid bilayer can be controlled by adjusting the droplet size. Further details of monolayer interfacial tension measurement, water permeability measurement, and adhesion energy measurement are summarized in the Supplementary Information.

References

1. McConnell, H. M. & Kornberg, R. D. Inside-outside transitions of phospholipids in vesicle membranes. *Biochemistry* **10,** 1111–1120 (1971).
2. Pautot, S., Frisken, B. J. & Weitz, D. Engineering asymmetric vesicles. *Proceedings of the National Academy of Sciences* **100,** 10718–10721 (2003).
3. Sackmann, E. Supported membranes: scientific and practical applications. *Science* **271,** 43 (1996).
4. Groves, J. T., Ulman, N. & Boxer, S. G. Micropatterning fluid lipid bilayers on solid supports. *Science* **275,** 651–653 (1997).
5. Yee, C. K., Amweg, M. L. & Parikh, A. N. Direct photochemical patterning and refunctionalization of supported phospholipid bilayers. *Journal of the American Chemical Society* **126,** 13962–13972 (2004).
6. Mueller, P., Rudin, D. O., Ti Tien, H. & Wescott, W. C. Reconstitution of cell membrane structure *in vitro* and its transformation into an excitable system. *Nature* **194,** 979–980 (1962).
7. Montal, M. & Mueller, P. Formation of bimolecular membranes from lipid monolayers and a study of their electrical properties. *Proceedings of the National Academy of Sciences* **69,** 3561–3566 (1972).
8. White, S., Petersen, D., Simon, S. & Yafuso, M. Formation of planar bilayer membranes from lipid monolayers. a critique. *Biophysical journal* **16,** 481 (1976).
9. White, S. Formation of "solvent-free" black lipid bilayer membranes from glyceryl monooleate dispersed in squalene. *Biophysical journal* **23,** 337–347 (1978).
10. Hennesthal, C. & Steinem, C. Pore-spanning lipid bilayers visualized by scanning force microscopy. *Journal of the American Chemical Society* **122,** 8085–8086 (2000).
11. Han, X. *et al.* Nanopore arrays for stable and functional free-standing lipid bilayers. *Advanced Materials* **19,** 4466–4470 (2007).
12. Ganesan, P. V. & Boxer, S. G. A membrane interferometer. *Proceedings of the National Academy of Sciences* **106,** 5627–5632 (2009).
13. Mey, I. *et al.* Local membrane mechanics of pore-spanning bilayers. *Journal of the American Chemical Society* **131,** 7031–7039 (2009).
14. Suzuki, H., Tabata, K., Kato-Yamada, Y., Noji, H. & Takeuchi, S. Planar lipid bilayer reconstitution with a micro-fluidic system. *Lab on a Chip* **4,** 502–505 (2004).
15. Funakoshi, K., Suzuki, H. & Takeuchi, S. Lipid bilayer formation by contacting monolayers in a microfluidic device for membrane protein analysis. *Analytical chemistry* **78,** 8169–8174 (2006).
16. Malmstadt, N., Nash, M. A., Purnell, R. F. & Schmidt, J. J. Automated formation of lipid-bilayer membranes in a microfluidic device. *Nano letters* **6,** 1961–1965 (2006).
17. Stachowiak, J. C. *et al.* Unilamellar vesicle formation and encapsulation by microfluidic jetting. *Proceedings of the National Academy of Sciences* **105,** 4697–4702 (2008).
18. Holden, M. A., Needham, D. & Bayley, H. Functional bionetworks from nanoliter water droplets. *Journal of the American Chemical Society* **129,** 8650–8655 (2007).
19. Thiam, A. R., Bremond, N. & Bibette, J. Adhesive emulsion bilayers under an electric field: from unzipping to fusion. *Physical review letters* **107,** 068301 (2011).
20. Thiam, A. R., Bremond, N. & Bibette, J. From stability to permeability of adhesive emulsion bilayers. *Langmuir* **28,** 6291–6298 (2012).
21. Leptihn, S. *et al.* Constructing droplet interface bilayers from the contact of aqueous droplets in oil. *Nature protocols* **8,** 1048–1057 (2013).
22. Thompson, J. R., Heron, A. J., Santoso, Y. & Wallace, M. I. Enhanced stability and fluidity in droplet on hydrogel bilayers for measuring membrane protein diffusion. *Nano letters* **7,** 3875–878 (2007).
23. Boreyko, J. B., Polizos, G., Datskos, P. G., Sarles, S. A. & Collier, C. P. Air-stable droplet interface bilayers on oil-infused surfaces. *Proceedings of the National Academy of Sciences* **111,** 7588–7593 (2014).
24. Gornall, J. L. *et al.* Simple reconstitution of protein pores in nano lipid bilayers. *Nano letters* **11,** 3334–3340 (2011).

25. Castellana, E. T. & Cremer, P. S. Solid supported lipid bilayers: From biophysical studies to sensor design. *Surface Science Reports* **61,** 429–444 (2006).
26. Edidin, M. Lipids on the frontier: a century of cell-membrane bilayers. *Nature Reviews Molecular Cell Biology* **4,** 414–418 (2003).
27. Simons, K. & Vaz, W. L. Model systems, lipid rafts, and cell membranes 1. *Annu. Rev. Biophys. Biomol. Struct.* **33,** 269–295 (2004).
28. Bloom, M., Evans, E. & Mouritsen, O. G. Physical properties of the fluid lipid-bilayer component of cell membranes: a perspective. *Quarterly reviews of biophysics* **24,** 293–397 (1991).
29. Honigmann, A., Walter, C., Erdmann, F., Eggeling, C. & Wagner, R. Characterization of horizontal lipid bilayers as a model system to study lipid phase separation. *Biophysical journal* **98,** 2886–2894 (2010).
30. Hansen, J. S., Thompson, J. R., Hélix-Nielsen, C. & Malmstadt, N. Lipid directed intrinsic membrane protein segregation. *Journal of the American Chemical Society* **135,** 17294–17297 (2013).
31. Veatch, S. L. & Keller, S. L. Separation of liquid phases in giant vesicles of ternary mixtures of phospholipids and cholesterol. *Biophysical journal* **85,** 3074–3083 (2003).
32. Collins, M. D. & Keller, S. L. Tuning lipid mixtures to induce or suppress domain formation across leaflets of unsupported asymmetric bilayers. *Proceedings of the National Academy of Sciences* **105,** 124–128 (2008).
33. Filippov, A., Orädd, G. & Lindblom, G. Influence of cholesterol and water content on phospholipid lateral diffusion in bilayers. *Langmuir* **19,** 6397–6400 (2003).
34. Poulin, P. & Bibette, J. Adhesion of water droplets in organic solvent. *Langmuir* **14,** 6341–6343 (1998).
35. Leal-Calderon, F., Schmitt, V. & Bibette, J. *Emulsion science: basic principles* (Springer Science & Business Media, 2007).
36. Mabrey, S. & Sturtevant, J. M. Investigation of phase transitions of lipids and lipid mixtures by sensitivity differential scanning calorimetry. *Proceedings of the National Academy of Sciences* **73,** 3862–3866 (1976).
37. Alvarez, N. J., Walker, L. M. & Anna, S. L. A non-gradient based algorithm for the determination of surface tension from a pendant drop: Application to low bond number drop shapes. *Journal of colloid and interface science* **333,** 55–562 (2009).
38. Hunter, D. & Frisken, B. Effect of extrusion pressure and lipid properties on the size and polydispersity of lipid vesicles. *Biophysical journal* **74,** 2996–3002 (1998).
39. Rawicz, W., Smith, B., McIntosh, T., Simon, S. & Evans, E. Elasticity, strength, and water permeability of bilayers that contain raft microdomain-forming lipids. *Biophysical journal* **94,** 4725–4736 (2008).
40. Mathai, J. C., Tristram-Nagle, S., Nagle, J. F. & Zeidel, M. L. Structural determinants of water permeability through the lipid membrane. *The Journal of general physiology* **131,** 69–76 (2008).

Acknowledgements

Author Contributions

D.-W. Jeong, S. Q. Choi and M. C. Choi conceived and designed the experiments; D.-W. Jeong performed experiments and analyzed data except interfacial tension measurement; H. Jang performed interfacial tension measurement and analyzed data; D.-W. Jeong, S. Q. Choi and M. C. Choi co-wrote the paper.

Additional Information

Supplementary information accompanies this paper at http://www.nature.com/srep

Competing financial interests: The authors declare no competing financial interests.

How to cite this article: Jeong, D.-W. *et al.* Enhanced stability of freestanding lipid bilayer and its stability criteria. *Sci. Rep.* **6,** 38158; doi: 10.1038/srep38158 (2016).

Publisher's note: Springer Nature remains neutral with regard to jurisdictional claims in published maps and institutional affiliations.